Spatial analysis of supraglacial debris cover in Svalbard, Arctic Region—a decadal study

Geetha Priya Murugesan[1] · Varshini Narayan[2] · Suresh Devaraj[3]

Abstract

Continental glacier melts directly influence the environment, resulting in sea-level rise affecting the settlements along the coast. The increase in global warming and constant change in the glacier mass grabbed the attention of researchers in understanding the evolution and distribution of glaciers. Despite the increase in the number of glacier studies, the difficulty is experienced by the researchers in understanding the supra-glacial debris cover and its characteristics. Supraglacial debris cover affects surface melt by increasing and decreasing ablation under thin and thick debris cover. In the present study, estimation of supraglacial debris cover (SDC) over Austre Brøggerbreen and Vestre Brøggerbreen glaciers of Ny-Ålesund is carried out with the aid of Landsat 5/7/8 datasets between 2000 and 2020. Supraglacial debris-cover is mapped using NDSI and band ratio techniques based on thresholding and it is estimated that Austre Brøggerbreen and Vestre Brøggerbreen glaciers are covered by 7.29% and 15.19% of SDC respectively. Results obtained are validated by a field visit to Arctic glacier, which is the first of its kind enhancing India's scientific credentials in Polar research.

Keywords Supraglacial debris cover · Svalbard · NDSI · NIR/SWIR · Decadal change

Introduction

A glacier is an enormous mass of ice that moves slowly over land. Glaciers are significant indicators of global warming and climate change in several ways. According to the National geographic society and National snow and ice data center (NSIDC), melting glaciers and ice sheets in Antarctica, the Arctic, and Greenland contribute to the rise in sea levels (Budikova 2009). Also, the impact of global warming is more in the Arctic compared to other parts of the world. Arctic habitats and populations are rapidly at risk due to increased warming and diminishing sea ice, according to the annual Arctic Report Card of the US National Atmospheric and Oceanic Administration (Mustonen et al. 2015). The Cryosphere requires extensive adaptation and mitigation action as all the Arctic and high mountain regions are facing wide-reaching variations as per the World Meteorological Organization, a specialized agency of the United Nations. Monitoring of the Cryosphere as glaciers are very vulnerable to climate change is a significant feature in Earth observation (Nuth et al. 2019). They undergo changes in physical properties like albedo, debris cover, mass balance, and ice velocity (Ranzi et al. 2004).

The glaciers with the ablation zone partly or fully covered with supraglacial debris (Hewitt 2014) are known as debris-covered glaciers. The extensive supraglacial debris cover alters the rates and spatial patterns of glacier melting. The lithological structure of debris replicates the excrescence outcrops that accelerate the melting of underlying ice (Gobbi et al. 2010; Benn et al. 2012). Glaciers in complex geological catchments can show compositional "striping" that can affect glacier albedo and energy balance (Shroder et al. 2000; Reznichenko et al. 2011). Black glaciers or debris-covered glaciers have surface temperatures a few degrees colder compared to pure debris on rocks. Hence, the debris superimposed on ice protects the glaciers from faster melting (Ranzi et al. 2004). Decadal studies on the supraglacial debris cover have

✉ Geetha Priya Murugesan
  geetha.sri82@gmail.com

[1] SENSE, Vellore Institute of Technology, Chennai 600127, India

[2] Department of ECE, Jyothy Institute of Technology, Thataguni, Bengaluru 560082, India

[3] CIIRC, Jyothy Institute of Technology, Thataguni, Bengaluru 560082, India

shown that glaciers are retreating. The proliferation of debris cover regions often results in glacier fragmentation and ice loss that may be induced by climate change (Pratibha and Kulkarni 2018). The existence of debris on the surface of the glacier has a very good influence over glacier surface energy and mass fluxes modifying surface energy environments by sharing heat with near-surface meteorological fields at lower elevations (Marshall et al. 2007). Rain transfers heat from the supraglacial debris to the ice or snow surface that influences ablation (Reid et al. 2012). The condensed surface melt of the avalanche-covered rock glacier can thicken due to slow ablation. The presence of meter-deep rock avalanche debris over the ablation zone directly impacts the mass balance and thus the motion of the glacier (Reznichenko et al. 2011; Collier et al. 2015). The behavior of glaciers has become less climate-dependent as debris affects the reduction of ablation levels (Hewitt et al. 2008).

Debris affects ablation, topography, and hydrological processes of glaciers impacting the supraglacial water chemistry, but the unstable subglacial network under the debris-covered region often plays a part in raising the contribution of ion to the proglacial stream (Fyffe et al. 2019). Supraglacial debris affects the rate of melting of glaciers and the spatial pattern of mass loss. Widespread debris also promotes the development of active terminus regions (Zhang et al. 2016). Debris-covered glaciers may contribute to the creation of large moraine-dammed lakes triggering glacier lake floods (GLOFs) (Nagai et al. 2013). Abandoning supraglacial debris can contribute to an overestimation of mass losses during the ablation season (Gardner et al. 2009; Collier et al. 2015). In recent years, owing to further ice loss due to global warming, the coverage of the supraglacial debris needs to be tracked. This paper focuses on the analysis of the supraglacial debris provided by satellite datasets of the Landsat sequence between 2000 and 2020 for Austre Brøggerbreen and Vestre Brøggerbreen glaciers of the Svalbard archipelago in the Arctic Ocean using the Normalized Difference Snow Index (NDSI) and the algorithm for NIR and SWIR band ratio, and the SDC region was mapped. The system of band ratio is not impaired by topographical conditions and could detect snow even under the shadow of mountains. Supervised classification-based methods consume greater post-processing time and sometimes may result in misclassification of pixels for snow under shadow.

Study area

Svalbard, an archipelago in the Arctic Ocean, comprises three major islands, Edgeøya, Nordaustlandet, and Spitsbergen, occupying a gross region of 62,700 km^2 and 60% of the territory occupied by glaciers. Ny-Ålesund is located on the western coast of the Svalbard archipelago in the Arctic Ocean (Fig. 1).

Ny-Ålesund has complex climate patterns that may supply evidence of climate change in the Arctic. This area with a humid climate sometimes may result in winter daily mean temperatures exceeding 0 °C due to North Atlantic warming current (Maturilli et al. 2013; Ding et al. 2018). The two glaciers, Austre Brøggerbreen (78° 51′ 35.892″ N 11° 49′ 44.0076″ E) and Vestre Brøggerbreen (78° 53′ 50.5428″ N11° 40′ 14.7396″ E) of Ny-Ålesund, are adopted as test sites to carry out the supraglacial debris cover study. Austre Brøggerbreen is a valley glacier with a surface area of 9.81 sq.km (RGI Consortium 2012) and is located in the northwestern part of Ny-Ålesund. Vestre Brøggerbreen glacier with a surface area of approximately 4.64 sq.km is a NE flowing small valley glacier (Patel et al. 2019). The average annual precipitation at the nearby weather station located at Ny-Ålesund (40 a.m.a.s.l.) is just under 400 mm depending on the world glacier monitoring service (wgms).

Materials and methods

Multispectral Landsat satellite scenes of Landsat-5 Thematic Mapper (TM) Sensor, Landsat-7 Enhanced Thematic Mapper (ETM+) sensor, and Landsat-8 Operational Land Imager (OLI) sensor were downloaded from http://earthexplorer. usgs.gov website for the years 2000, 2002, 2005, 2007, 2009, 2013, 2014, 2016, 2017, 2018, 2019, and 2020 covering the study period (2000–2020). The data with the least cloud cover and snow were selected during the ablation season of every year. Landsat series of satellites have a revisit period of 16 days (Reddy et al. 2019). Green, short-wave infrared (SWIR) and near-infrared (NIR) bands with 30-m spatial resolution are used for the present study to estimate the NDSI and NIR/SWIR band ratios (Fig. 2). The scan line errors of Landsat-7 data (acquired post 31st May 2003) were corrected (Markham and Barker 1986; Storey et al. 2005) during pre-processing of the datasets. The selection of the data acquisition period is based on data availability during the ablation season with August, September, and July as the order of preference (data gap for the years 2001, 2003, 2004, 2006, 2008, 2010, 2011, and 2012 is due to non-availability of data/cloud-free data during ablation season) (Table 1). The Randolph Glacier Inventory (RGI Consortium 2012) provides a regional database of glacier diagrams and is used for the glacier boundary.

Data pre-processing

The data downloaded from the USGS earth explorer website is available in the form of digital numbers (DN). Radiometric errors are caused due to incorrect luminance values in pixels recorded in an image (Chander et al. 2009). To overcome the radiometric error caused by atmospheric conditions, the

Fig. 1 Location of glaciers in Svalbard archipelago
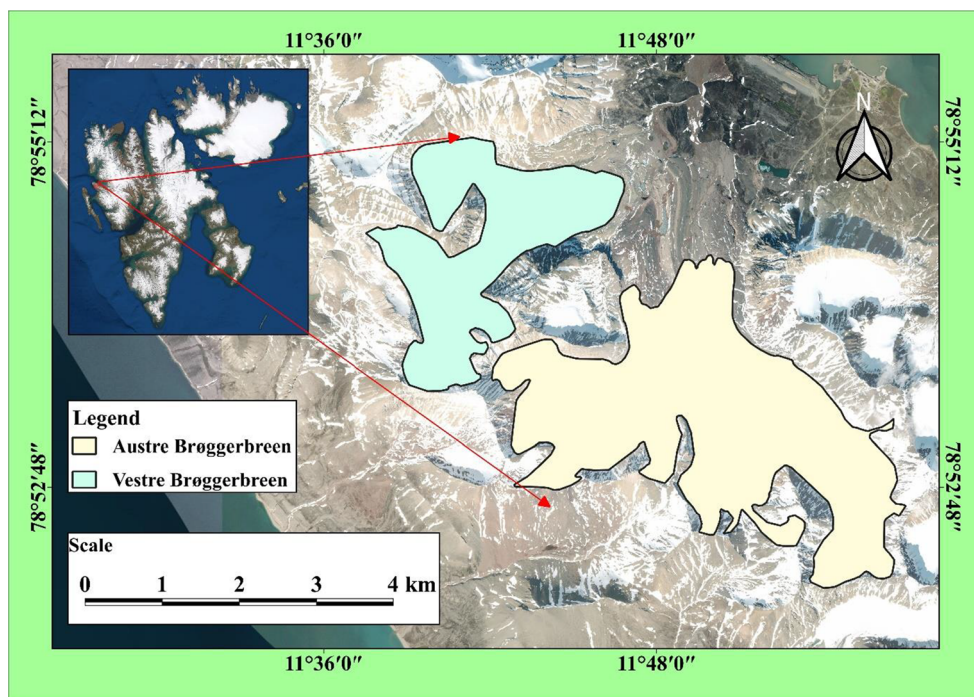
digital numbers are transformed into spectral radiance and the spectral radiance is transformed to the top of the atmospheric reflectance (TOA) using Eqs. 1 and 2 respectively. Landsat-7 datasets were pre-processed after scan line error corrections.

$$L_\lambda = M_L * Q_{cal} + A_L \tag{1}$$

$$\rho_\lambda = M_\rho * Q_{cal} + A_\rho \tag{2}$$

Where L_λ is the spectral radiance, M_L is the band-specific radiance multiplicative rescaling factor, A_L is the band-specific additive rescaling factor from the metadata, ρ_λ is the ToA reflectance, M_ρ is the band-specific reflective multiplicative rescaling factor from the meta data, Q_{cal} is the quantized and calibrated standard product pixel value, and A_ρ is the band-specific additive rescaling factor from metadata.

Spectral indexing and band ratioing

The post-processing is performed to find the SDC area of the glacier using the Normalized Difference Snow Index (NDSI) (Kulkarni et al. 2002) and NIR-SWIR (Paul et al. 2002) band ratio techniques. NDSI shown in Eq. 3 is a very useful well-established snow cover mapping technique that differentiates snow from the cloud with the capability to map even snow cover under mountain shadow. As snow/ice has high reflectance in visible bands and low reflectance in SWIR bands, band ratioing of these bands with appropriate thresholding is

Table 1 List of Landsat datasets used in the present study

Scene ID	Date	Path no.	Row no.
LE07_L1TP_220003_20000726_20201008_02_T	26 July 2000	220	3
LE07_L1TP_217003_20020711_20200916_02_T1	11 July 2002	217	3
LT05_L1TP_216004_20060723_20201008_02_T1	23 July 2005	216	4
LE07_L1TP_220003_20070714_20200913_02_T1	14 July 2007	220	3
LE07_L1GT_223002_20090724_20161219_01_T2	24 July 2009	223	2
LC08_L1TP_217003_20130919_20170502_01_T1	19 Sep 2013	217	3
LC08_L1TP_028241_20140825_20170420_01_T2	25 Aug 2014	28	241
LC08_L1TP_216004_20160702_20170323_01_T1	9 July 2016	217	3
LC08_L1TP_220003_20170802_20170812_01_T1	2 Aug 2017	221	3
LC08_L1TP_023241_20180801_20180814_01_T2	1 Aug 2018	23	241
LC08_L1TP_022241_20190728_20190801_01_T1	28 July 2019	22	241
LC08_L1TP_218003_20200727_20200908_02_T1	27 July 2020	218	3

Fig. 2 Flow diagram for mapping SDC
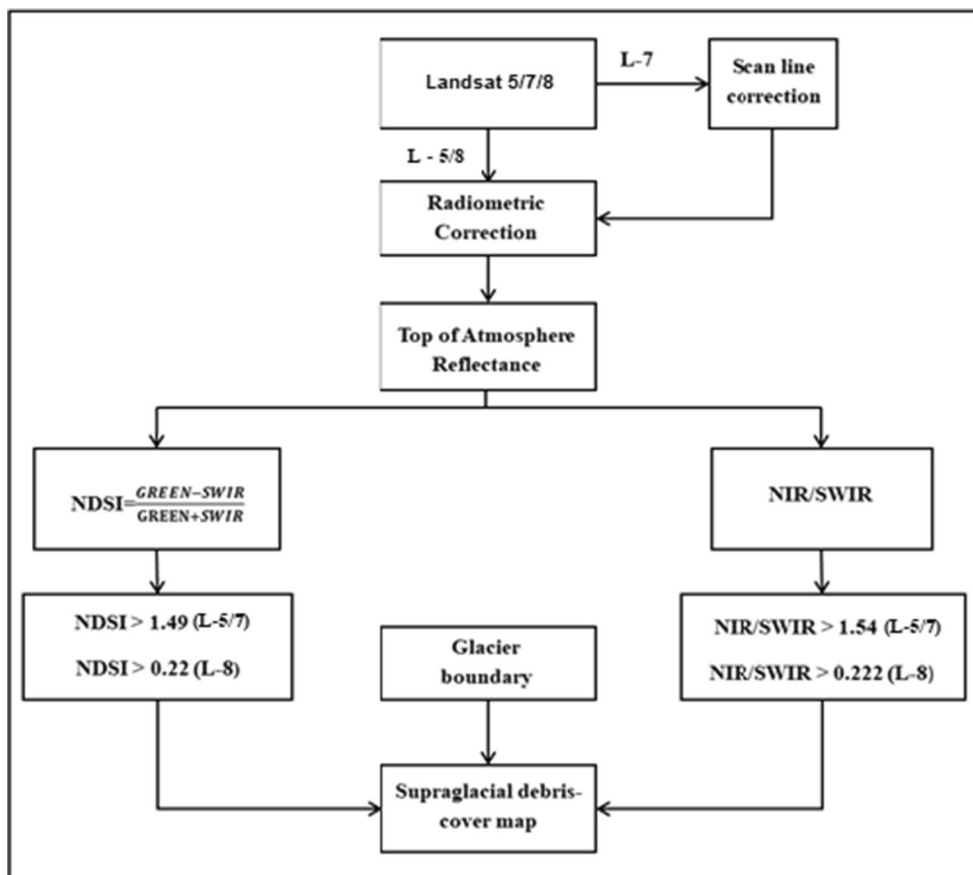
made for mapping the snow cover (Racoviteanu and Williams 2012; Sahu and Gupta 2018) and (Paul et al. 2002) has found that NDSI and NIR/SWIR ratio are the best techniques for glacier mapping respectively as these methods are not influenced by (Pratibha and Kulkarni 2018) topographic conditions.

$$NDSI = \frac{GREEN\ Reflectance - SWIR\ Reflectance}{GREEN\ Reflectance + SWIR\ Reflectance} \quad (3)$$

Mapping supraglacial debris cover

As the field-based studies are difficult and not logistically feasible every time, we use remote sensing techniques to collect information over large spatial areas, characterize the features like debris on glaciated regions, and monitor Cryosphere changes over the years. Different thresholds were applied on NDSI and NIR/SWIR ratios computed separately for Landsat-5, Landsat-7, and Landsat-8 pre-processed TOA datasets. The NDSI and NIR/SWIR thresholds used for Landsat-8 are 0.222 and 1.54 respectively. Similarly, for Landsat 5 and 7, NDSI and NIR/SWIR thresholds are 0.22 and 1.49 respectively (Pratibha and Kulkarni 2018). On applying suitable threshold values for NDSI and NIR/SWIR band ratio, the snow/ice-covered and debris-covered areas are obtained. The glacier

boundary extent is obtained by clipping the post-processed data on overlaying the GLIMS RGI V2.0 polygons. The GLIMS RGI V2.0 glacier boundaries of Austre Brøggerbreen and Vestre Brøggerbreenare were manually modified using satellite imagery of 2016 and used throughout the study period for estimation of supraglacial debris cover (Bolch et al. 2010; Bhambri et al. 2011; Karimi et al. 2012; Sahu and Gupta 2020)

Results and discussion

Remote sensing is the progression of sensing, monitoring, and obtaining information about objects or areas from distance by computing its reflected and emitted radiation (Campbell and Wynne 2011). The proposed study was carried out on two glaciers, Austre Brøggerbreen (AB) and Vestre Brøggerbreen (VB) for the analysis of decadal change in the SDC area over the years 2000–2020. The glacier areas according to the manually modified glacier boundary are 9.81 sq.km and 4.64 sq.km. Figures 3 and 4 represent the SDC maps of Austre Brøggerbreen and Vestre Brøggerbreen glaciers respectively. For the estimation of SDC area, only the manually delineated ablation region of the two glaciers is considered. The average estimated SDC area using NDSI and NIR/SWIR

band ratio techniques for the years 2000, 2002, 2005, 2007, 2009, 2013, 2014, 2016, 2017, 2018, 2019, and 2020 are shown in Table 2 for the two glaciers. NDSI provides a clean glacier mapping separating the ice-covered area and debris-covered area, whereas the NIR/SWIR band ratio also gives a best-suited glacier mapping.

From Table 2, the following inferences are made for AB glacier:

- The average SDC area of Austre Brøggerbreen glacier is approximately 0.36% (less than 1%) and 7.29% in July 2000 and July 2020 respectively covering the study period 2000–2020.
- A maximum SDC area of around 9.53–9.79% has been estimated for August 2017 and August 2018 respectively.
- For August 2014, a minimum SDC area of about 2.55% was obtained, followed by 4.84% in July 2016 and 5.96%

in July 2016 and September 2013 for the period 2011–2020.

It was found that the SDC area differed significantly from the year 2009 (6.63%), while less than 2% of the SDC area was seen during the years 2000–2007. From Table 2, the following inferences are made for VB glacier:

- The average SDC area of Vestre Brøggerbreen glacier is approximately 1.08% and 15.19% in July 2000 and July 2020 respectively covering the study period 2000–2020.
- A maximum SDC area of around 15.19% has been estimated for July 2020 followed by 14.66% in August 2017, 13.69% in July 2019, and 12.93% in August 2018.
- A minimum SDC area of less than 1% (i.e., 0.75%) is obtained for August 2014.

Table 2 Supraglacial debris (SDC) area resulting from the combination of NDSI and NIR/SWIR algorithms for Austre Brøggerbreen and Vestre Brøggerbreen

Austre Brøggerbreen (9.81 sq.km)

Year	NDSI-based SDC area (sq.km)	NIR/SWIR-based SDC area (sq.km)	Average area of SDC (sq.km)	Average area of SDC (%)
July 2000	0.04	0.03	0.04	0.36%
July 2002	0.02	0.02	0.02	0.20%
July 2005	0.19	0.18	0.19	1.89%
July 2007	0.13	0.12	0.13	1.27%
July 2009	0.66	0.64	0.65	6.63%
Sep 2013	0.53	0.64	0.59	5.96%
Aug 2014	0.26	0.24	0.25	2.55%
July 2016	0.47	0.48	0.48	4.84%
Aug 2017	0.89	0.98	0.94	9.53%
Aug 2018	0.92	1.00	0.96	9.79%
July 2019	0.75	0.8	0.78	7.90%
July 2020	0.71	0.72	0.72	7.29%

Vestre Brøggerbreen (4.64 sq.km)

| Year	NDSI-based SDC area (sq.km)	NIR/SWIR-based SDC area (sq.km)	Average area of SDC (sq.km)	Average area of SDC (%)
July 2000	0.05	0.05	0.05	1.08%
July 2002	0.08	0.07	0.08	1.62%
July 2005	0.14	0.13	0.14	2.91%
July 2007	0.04	0.04	0.04	0.86%
July 2009	0.43	0.51	0.47	10.13%
Sep 2013	0.39	0.44	0.42	8.94%
Aug 2014	0.03	0.04	0.04	0.75%
July 2016	0.40	0.41	0.41	8.73%
Aug 2017	0.67	0.69	0.68	14.66%
Aug 2018	0.59	0.61	0.60	12.93%
July 2019	0.63	0.64	0.64	13.69%
July 2020	0.69	0.72	0.71	15.19%
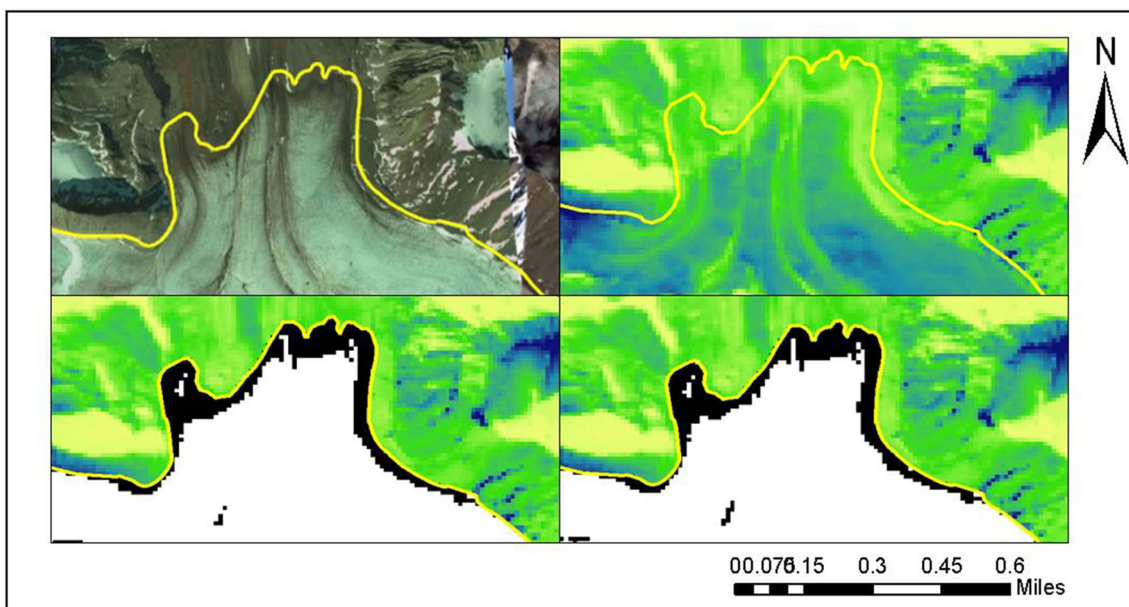
Fig. 3 Validation of the AB glacier study. (a) Google Earth Photo (July 2016) of SDC at the terminus of AB Glacier. (b) FCC of NIR, SWIR1, and SWIR2 of Landsat Imagery of July 2017. (c) SDC region obtained from NDSI. (d) SDC region by NIR and SWIR ratio

- An average SDC area of 8.82–9.04% has been estimated for July 2016 and September 2013 respectively
- It was found that the SDC area differed significantly from the year 2009 (10.13%), while less than 3% of the SDC area was seen during the years 2000–2007.

The estimations made during August are more preferred compared to July or September estimations. This is because the ablation region is exposed completely due to increased melting during the August month of every hydrological year (HY), whereas September month may experience sudden
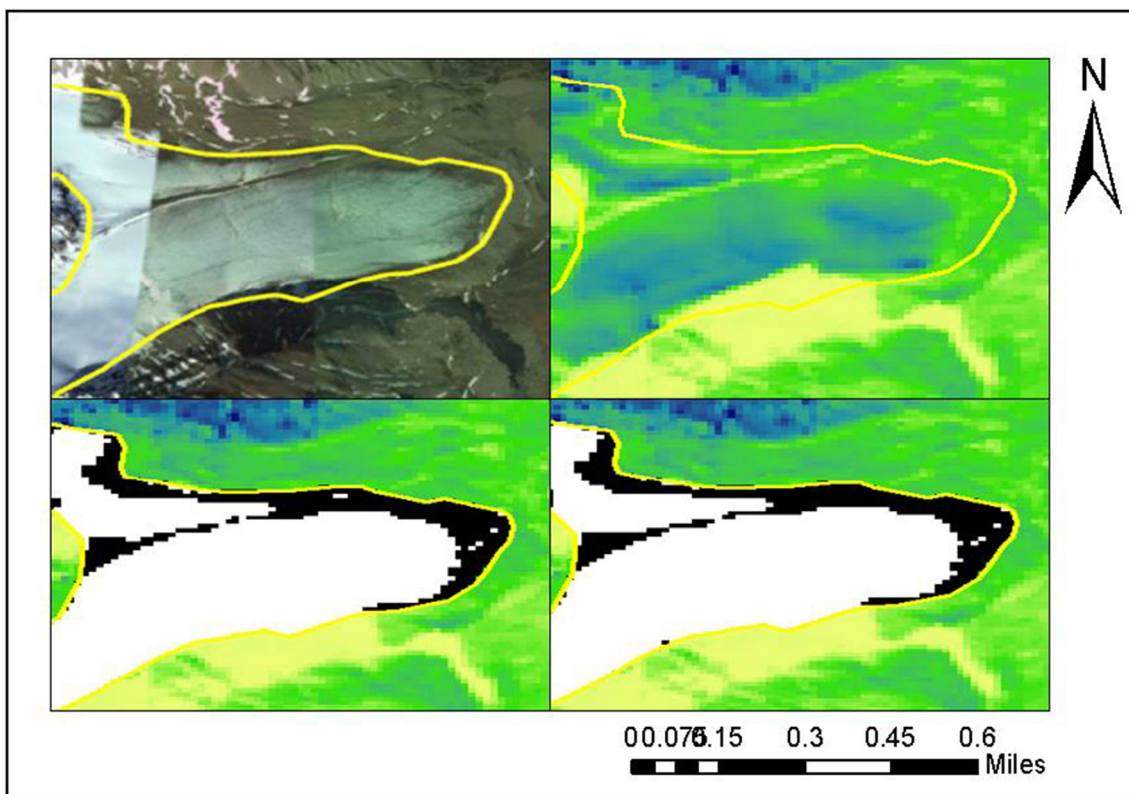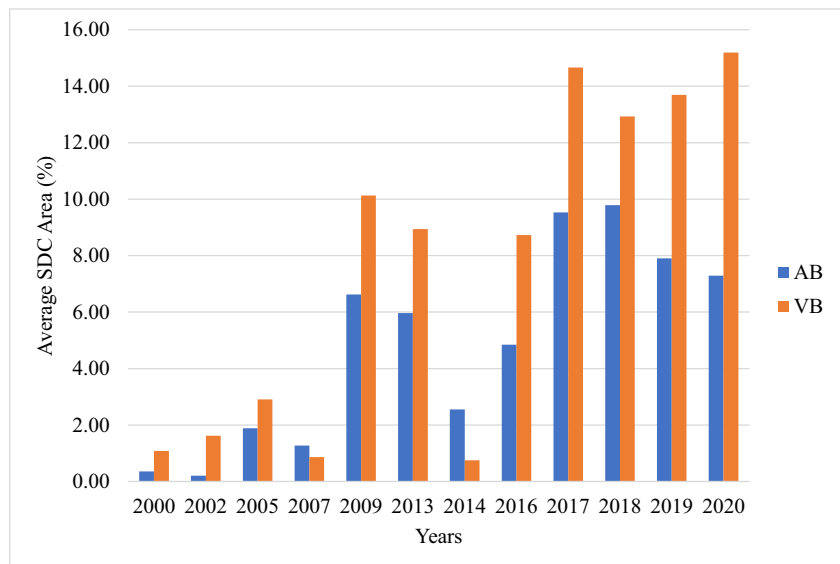

Fig. 4 Validation of the VB glacier study. (a) Google Earth photo (July 2016) of SDC near the terminus of VB Glacier. (b) FCC of the NIR, SWIR1, and SWIR2 bands of Landsat Imagery of July 2017. (c) SDC region derived from NDSI. (d) SDC region by NIR and SWIR ratio

Fig. 5 Average SDC area for AB and VB glaciers for the study period 2000–2020

snowfall and a part of the ablation region remains snow-covered. Similarly, in July month, a part of the ablation region remains snow-covered due to less melting at the beginning of the ablation season. Figure 5 indicates that the minimum SDC was observed for the two glaciers prior to 2009 and August 2014. This could be due to much more solid snow or much less melting that mimics the progression of the glacier prior to 2009 and during 2014. Also, satellite data is not available for the year 2014 during June, July, and September due to the data gap/cloud cover to validate this specific event. Another possibility is that repeated spells of snowfall on the day of satellite data acquisition will result in less SDC areas in the event of snowfall. However, there is an increase in the SDC area for the years 2016–2019 indicating the recession of the two glaciers.

Figure 6 shows the validation of the proposed study of debris cover at Vestre Brøggerbreen glacier (Ground Control Point 78° 54′ 50.75″ N, 11° 46′ 14.39″ E). National Centre Polar and Ocean Research, Ministry of Earth Sciences, Government of India, Goa in collaboration with Norwegian Government has supported the logistical access to Ny-Alesund, Svalbard, Arctic to carry out this scientific research work during September 2019.

Decadal analysis of the SDC area shows that there is an increase in the average SDC area of up to 6.93% and 14.11% for both Austre Brøggerbreen and Vestre Brøggerbreen glaciers at the start and end of the study period 2000–2020 respectively. The estimated figures of the SDC area can also be used to understand the rate of rockfall in a given glacier. The

Fig. 6 Debris cover validated at Vestre Brøggerbreen glacier during September 2019—Ground Control Point 78° 54′ 50.75″ N, 11° 46′ 14.39″ E

increase of the SDC area may contribute to the negative mass balance of the glacier. Due to ice loss occurrence, the larger glaciers may split leading to glacier fragmentation (Jia et al. 2020). Based on reported values, it can be said that these glaciers are partially debris-covered.

Conclusion

This study was carried out using the available satellite data downloaded from USGS with an approach of studying the decadal change in the debris-covered area for two of the glaciers in the Svalbard archipelago for the years 2000–2020. Thresholding of NDSI and NIR/SWIR band ratioing techniques were considered to separate the ice- and debris-covered areas using the available thresholds. Study results show an increase in the SDC area mapped indicating the snow and ice loss over a decade from the glaciers. Based on this study, the glaciers can be called partially debris-covered glaciers with large accumulation areas. The present SDC analysis can be combined in the mass balance model as this forecasts potential mass losses related to climate change.

Author contributions Geetha Priya Mursugesan conceptualized the idea, and provided the necessary resources to carry out this research and supervised Varshini Narayan and Suresh Devaraj throughout this study. Varshini Narayan processed and analyzed the datasets. Geetha Priya Murugesan and Suresh Devaraj wrote the manuscript. Suresh Devaraj provided essential technical inputs that helped improve the manuscript.

Data availability The dataset utilized/analyzed during the current study will be available from the corresponding author upon request.

Compliance with ethical standards

Competing interests The authors declare that they have no competing interests.

Ethical statement All ethical practices have been followed in relation to the development, data analysis, writing, and publication of this research article.

Consent to participate Consent to participate is "Not applicable" for the manuscript.

Consent to publish The datasets used in the present study are open-access datasets downloaded from USGS Earth explorer, and the results are generated by the author in the laboratory. None of the data used belongs to any person in any form.

References

Benn DI, Bolch T, Hands K et al (2012) Response of debris-covered glaciers in the Mount Everest region to recent warming, and implications for outburst flood hazards. Earth-Science Rev 114:156–174. https://doi.org/10.1016/j.earscirev.2012.03.008

Bhambri R, Bolch T, Chaujar RK, Kulshreshtha SC (2011) Glacier changes in the Garhwal Himalaya, India, from 1968 to 2006 based on remote sensing. J Glaciol 57:543–556. https://doi.org/10.3189/002214311796905604

Bolch T, Menounos B, Wheate R (2010) LANDSAT-based inventory of glaciers in Western Canada, 1985–2005. Remote Sens Environ 114:127–137. https://doi.org/10.1016/j.rse.2009.08.015

Budikova D (2009) Role of Arctic sea ice in global atmospheric circulation: a review. Glob Planet Chang 68:149–163. https://doi.org/10.1016/j.gloplacha.2009.04.001

Campbell JB, Wynne RH (2011) Introduction to remote sensing, 5th edn. The Guilford Press, New York

Chander G, Markham BL, Helder DL (2009) Summary of current radiometric calibration coefficients for Landsat MSS, TM, ETM+, and EO-1 ALI sensors. Remote Sens Environ 113:893–903. https://doi.org/10.1016/j.rse.2009.01.007

Collier E, Maussion F, Nicholson LI et al (2015) Impact of debris cover on glacier ablation and atmosphere–glacier feedbacks in the Karakoram. Cryosph 9:1617–1632. https://doi.org/10.5194/tc-9-1617-2015

Ding M, Wang S, Sun W (2018) Decadal climate change in Ny-Ålesund, Svalbard, a representative area of the Arctic. Condens Matter 3:12. https://doi.org/10.3390/condmat3020012

Fyffe CL, Brock BW, Kirkbride MP et al (2019) The impact of supraglacial debris on proglacial runoff and water chemistry. J Hydrol 576:41–57. https://doi.org/10.1016/j.jhydrol.2019.06.023

Gardner AS, Sharp MJ, Koerner RM et al (2009) Near-surface temperature lapse rates over Arctic glaciers and their implications for temperature downscaling. J Clim 22:4281–4298. https://doi.org/10.1175/2009JCLI2845.1

Gobbi M, Isaia M, De Bernardi F (2010) Arthropod colonisation of a debris-covered glacier. The Holocene 21:343–349. https://doi.org/10.1177/0959683610374885

Hewitt K (2014) Glaciers of the Karakoram Himalaya. In: Encyclopedia of snow, ice and glaciers. Springer, Dordrecht, pp 429–436

Hewitt K, Clague J, Orwin J (2008) Legacies of rock slope failures in mountain landscapes. Earth-Science Rev 87:1–38. https://doi.org/10.1016/j.earscirev.2007.10.002

Jia Y, Li Z, Jin S et al (2020) Runoff changes from Urumqi Glacier no. 1 over the past 60 years, Eastern Tianshan, Central Asia. Water (Switzerland) 12:1–15. https://doi.org/10.3390/W12051286

Karimi N, Farokhnia A, Karimi L et al (2012) Combining optical and thermal remote sensing data for mapping debris-covered glaciers (Alamkouh Glaciers, Iran). Cold Reg Sci Technol 71:73–83. https://doi.org/10.1016/j.coldregions.2011.10.004

Kulkarni AV, Srinivasulu J, Manjul SS, Mathur P (2002) Field based spectral reflectance studies to develop NDSI method for snow cover monitoring. J Indian Soc Remote Sens 30:73–80. https://doi.org/10.1007/BF02989978

Markham BL, Barker JL (1986) Landsat MSS and TM post-calibration dynamic rangers, exoatmospheric reflectance and at-satellite temperatures. EOSAT Landsat Tech Notes 3–8

Marshall SJ, Sharp MJ, Burgess DO, Anslow FS (2007) Near-surface-temperature lapse rates on the Prince of Wales Icefield, Ellesmere Island, Canada: implications for regional downscaling of temperature. Int J Climatol 27:385–398. https://doi.org/10.1002/joc.1396

Maturilli M, Herber A, König-Langlo G (2013) Climatology and time series of surface meteorology in Ny-Ålesund, Svalbard. Earth Syst Sci Data 5:155–163. https://doi.org/10.5194/essd-5-155-2013

Mustonen T, Jeffries M, Richter-Menge J, Overland J (2015) Arctic Report Card 2015

Nagai H, Fujita K, Nuimura T, Sakai A (2013) Southwest-facing slopes control the formation of debris-covered glaciers in the Bhutan Himalaya. Cryosph 7:1303–1314. https://doi.org/10.5194/tc-7-1303-2013

Nuth C, Gilbert A, Köhler A et al (2019) Dynamic vulnerability revealed in the collapse of an Arctic tidewater glacier. Sci Rep 9:5541. https://doi.org/10.1038/s41598-019-41117-0

Patel L, Sharma P, Thamban M (2019) Spatio-temporal variability of snow water equivalent over the Vestre Broggerbreen and Feiringbreen glaciers, Ny-Ålesund, Svalbard. J Earth Syst Sci 128:183. https://doi.org/10.1007/s12040-019-1224-4

Paul F, Kääb A, Maisch M et al (2002) The new remote-sensing-derived Swiss glacier inventory: I. Methods. Ann Glaciol 34:355–361. https://doi.org/10.3189/172756402781817941

Pratibha S, Kulkarni A (2018) Decadal change in supraglacial debris cover in Baspa basin, Western Himalaya. Curr Sci 114:792–799. https://doi.org/10.18520/cs/v114/i04/792-799

Racoviteanu A, Williams MW (2012) Decision tree and texture analysis for mapping debris-covered glaciers in the Kangchenjunga area, eastern Himalaya. Remote Sens 4:3078–3109

Ranzi R, Grossi G, Iacovelli L, Taschner S (2004) Use of multispectral ASTER images for mapping debris-covered glaciers within the GLIMS Project

Reddy KR, Devaraj S, Biradar S et al (2019) Spatial distribution of land use/land cover analysis in Hanamkonda taluk, Telangana - a case study. Indian J Geo-Marine Sci 48:1761–1768

Reid T, Carenzo M, Pellicciotti F, Brock B (2012) Including debris cover effects in a distributed model of glacier ablation. J Geophys Res 117:18105. https://doi.org/10.1029/2012JD017795

Reznichenko NV, Davies TRH, Alexander DJ (2011) Effects of rock avalanches on glacier behaviour and moraine formation. Geomorphology 132:327–338. https://doi.org/10.1016/j.geomorph.2011.05.019

RGI Consortium (2012) Randolph Glacier Inventory – a dataset of global glacier outlines: version 2.0: technical report. , Global Land Ice Measurements from Space, Colorado. Digital Media.

Sahu R, Gupta R (2018) Conceptual framework of combined pixel and object-based method for delineation of debris-covered glaciers. ISPRS Ann Photogramm Remote Sens Spat Inf Sci 173–180

Sahu R, Gupta RD (2020) Glacier mapping and change analysis in Chandra basin, Western Himalaya, India during 1971–2016. Int J Remote Sens 41:6914–6945. https://doi.org/10.1080/01431161.2020.1752412

Shroder JF, Bishop MP, Copland L, Sloan VF (2000) Debris-covered glaciers and rock glaciers in the Nanga Parbat Himalaya, Pakistan. Geogr Ann Ser A, Phys Geogr 82:17–31. https://doi.org/10.1111/j.0435-3676.2000.00108.x

Storey J, Scaramuzza P, Schmidt G (2005) Landsat 7 scan line corrector-off gap-filled product development. In: Pecora 16 "Global Priorities in Land Remote Sensing"

Zhang Y, Hirabayashi Y, Fujita K et al (2016) Heterogeneity in supraglacial debris thickness and its role in glacier mass changes of the Mount Gongga. Sci China Earth Sci 59:170–184. https://doi.org/10.1007/s11430-015-5118-2